Asociación Argentina
de Mecánica Computacional

Mecánica Computacional Vol XXXIII, págs. 2175-2183 (artículo completo)
Graciela Bertolino, Mariano Cantero, Mario Storti y Federico Teruel (Eds.)
San Carlos de Bariloche, 23-26 Setiembre 2014

VIBRATION-BASED ENERGY HARVESTING USING A LEAD-FREE PIEZOELECTRIC MATERIAL

Mariano Febbo[a], Sebastián P. Machado[b], Leandro A. Ramajo[c] and Miriam S. Castro[c]

[a]*Instituto de Física del Sur y Departamento de Física, Universidad Nacional del Sur, Avda. Alem 1253, 8000 Bahía Blanca, Buenos Aires, Argentina, mfebbo@uns.edu.ar* http://www.uns.edu.ar

[b]*Grupo de Análisis de sistemas mecánicos, Centro de Investigaciones de Mecánica Teórica y Aplicada, Universidad Tecnológica Nacional FRBB, 11 de Abril 461, 8000 Bahía Blanca, Buenos Aires, Argentina*

[c]*División Cerámicos, INTEMA, CONICET-UNMdP, Avda. Juan B. Justo 4302, B7068FDQ Mar del Plata, Buenos Aires, Argentina*

Keywords: Piezoelectric energy harvesting, lead-free piezoelectric material, analytical and experimental results.

Abstract. Vibration-based energy harvesting is visualized as an auxiliary power source, which can provide small amounts of energy to power remote sensors installed over inaccessible locations. The article presents an experimental and analytical investigation of an energy harvesting device using a lead-free piezoelectric material based on MoO_3-doped $(K_{0.44}Na_{0.52}Li_{0.04})(Nb_{0.86}Ta_{0.10}Sb_{0.04})O_3$ (KNL-NTS) obtained by the conventional solid state reaction. The harvesting model corresponds to a cantilever beam with a KNL-NTS piezoelectric disc attached to it subjected to base excitation. We analyze the effect of the electromechanical coupling and the load resistance on the output electrical power. Electromechanical frequency response functions (FRFs), that relate the voltage output to the translational base acceleration are shown for experimental and analytical results.

1 INTRODUCTION

Energy harvesting is one of the most promising techniques for a wide variety of self-powered systems. Among the energy harvesting sources, we can find solar power, thermal gradients and vibration (1). Last years, the attention of many researches have concentrated on mechanical vibration as a potential power source since it is abundant enough to be of use, it is easily accessible through microelectromechanical systems (MEMS) and it is ubiquitous in applications ranging from small household appliances to large infrastructures (2),(3).

Piezoelectric energy harvesting is one possibility of energy harvesting from mechanical vibrations as a power source (1). Its fundamental advantage lies in they have high electromechanical coupling which means a large strain/voltage conversion, require no external voltage source and are adequate to miniaturize (4), (5), (6).

In the vast majority of the applications, the most common type of piezoelectric used is lead zirconate titanate, known as PZT. However, a number of different piezoelectric materials have been developed. The type of piezoelectric material selected for a power harvesting application can have a major influence on the harvesters functionality and performance. Although PZT is widely used as a power harvesting material, the toxicity of lead is a serious threat to human health and the environment and thus lead-free piezoelectric ceramics have attracted great attention recently. Numerous studies on lead-free piezoelectric ceramics such as (K,Na)NbO_3, $BaTiO_3$-based, Bi-layered, bismuth sodium titanate and tungsten bronze-typematerials have been recently published (7), (8), (9). In this way, niobates (K,Na)NbO_3 (KNN)- based ceramics have shown good piezoelectric and electric properties, high Curie temperature and environmental inequity. When the ratio of K/Na reaches 50/50, the piezoelectric coefficient reaches the highest point (up to 80 pC/N) (10). This composition is reported to be composed of a virtual morphotropic phase boundary, where the total polarization can be maximized due to increased possibility of domain orientation. However, the exact crystallographic nature of this boundary in KNN is presently not well understood and it may be different than the one in lead-zirconate titanate solid solution (11). On the other hand, Saito *et. al.* (12) reported exceptionally high piezoelectric properties in the system (K,Na)NbO_3 $LiTaO_3$ $LiSbO_3$. This study was based on chemical modifications, in the vicinity of the MPB of (K,Na)NbO_3 (KNN), by complex simultaneous substitutions in the A (Li) and B (Ta and Sb) site of the perovskite lattice. In this way, similar composition with 4 mol % of Lithium and 10 mol % of tantalum substituted KNN ceramic prepared by simple pressureless solid state sintering without aid additives or special powder handling reach interesting properties with $d_{33} < 160$ pC/N without antimony (13). In this paper, MoO_3-doped lead-free $(K_{0.44}Na_{0.52}Li_{0.04})(Nb_{0.86-x}Ta_{0.1-x}Sb_{0.04-x})Mo_{5/6x}O_3$ (KNL NTS), was used as a new material to harvest vibration energy.

The aim of the present work is to analyze the power generation of a novel lead-free piezoelectric material under a vibration-based excited system.

First section introduces the state of the art and gives a description of the different type of piezoelectric transducers. After that, section 2 derives the mathematical formulation of the problem. Then, section 3 presents the results of the voltage generation and power of the electromechanical system as a function of the frequency of excitation. Finally, some concluding remarks are presented and discussed.

2 MATHEMATICAL DESCRIPTION AND MODELLING

The system under study comprises a lead free lead-free piezoelectric material based on MoO_3-doped $(K_{0.44}Na_{0.52}Li_{0.04})(Nb_{0.86}Ta_{0.10}Sb_{0.04})O_3$ (KNL-NTS) in the form of a disc, ob-

tained in Argentina at INTEMA attached to a steel beam which acts as its support (see Fig. 1). All the system is excited by its base over the form of a deterministic function $g(t)$ which try to mimic an environmental excitation from which energy can be extracted.

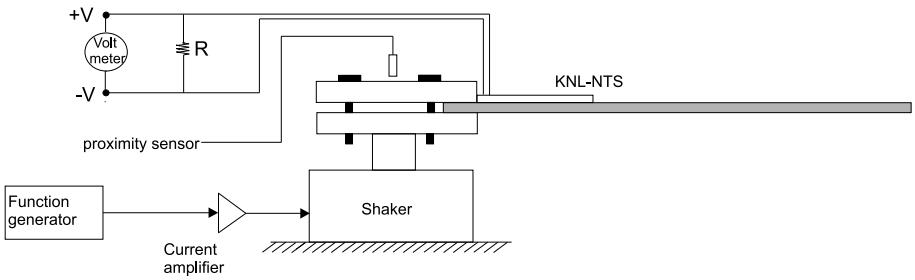

Figure 1: Schematic diagram of the experimental setup.

For the sake of brevity we refer to a previous paper by two of the authors (14) to see the derivation of the electromechanical equations that give the voltage generation and the beam displacement. These are:

$$\overline{v} = \frac{\Gamma_j \theta_j \Omega R}{\sqrt{(\omega_j^2 - \Omega^2 - 2CR\xi_j\omega_j\Omega^2)^2 + (2\Omega\xi_j\omega_j + R\Omega(\theta_j^2 + C\omega_j^2 - C\Omega^2))^2}} \tag{1}$$

and for the modal coordinate

$$\overline{\eta} = \frac{\Gamma_j \sqrt{1 + C^2R^2\Omega}}{\sqrt{(\omega_j^2 - \Omega^2 - 2CR\xi_j\omega_j\Omega^2)^2 + (2\Omega\xi_j\omega_j + R\Omega(\theta_j^2 + C\omega_j^2 - C\Omega^2))^2}} \tag{2}$$

where Γ_j is the modal coupling, θ_j is the piezoelectric coupling, Ω is the excitation frequency, R is the resistive load, ω_j is the j-th natural frequency of the vibrating system, C is the capacity of the piezoelectric disc and ξ_j is the j-th damping coefficient.

To obtain the electromechanical coupling we use an approximation. This consists in replacing the disc by a rectangle of the same area with its length equal to the diameter of the disc.

Then, the displacement field is given by: $w(x,t) = \sum_{k=1}^{2} \phi_{j,k}\overline{\eta}_j \, e^{i\Omega t}$.

3 EXPERIMENTS AND DISCUSSION

The aim of the present section is to compare the analytically obtained voltage function Eq.(1) with the voltage observed in the experiments. As we mentioned before, the excitation is provided by an electromechanical shaker. Base displacement is measured by a displacement proximity sensor and then converted into acceleration. The sinusoidal excitation is provided by a signal generator in a frequency sweep over the frequencies of interest and its power adjusted by a power amplifier. All measured signals are then filtered by a low pass-filter to recover them for postprocessing using a data acquisition system. (see Fig. 1). The actual setup for the experiment is illustrated in Fig. (2).

In Table (1) we present the physical and geometrical parameters of the steel beam and of the piezoceramic disc of KNL-NTS.

In the following, the experimental results are presented for the first two modes of the proposed system.

To make a useful comparison with other authors (see for example (15)), the voltage function of Eq.(1) is divided by base acceleration to obtain a voltage to base acceleration frequency

Table 1: Geometrical and physical parameters of the prototype device consisting in a steel beam and a piezoelectric disc used for the experiments.

Geometrical parameters	beam (steel)	piezoelectric disc (PZT)	Material parameters	beam (steel)	piezoelectric disc
Length, L (mm)	115.6	16.12 (diameter)	density ρ (kgm^{-3})	7800	4470
width, b (mm)	19	—	Young modulus, E (GPa)	210	105
thickness, b (mm)	0.9	1.96	piezo constant, d_{31} (pm V^{-1})	—	- 45 10^{-12}
mass M_t, (kg)	–	–	Capacity C (nF)	—	4.02

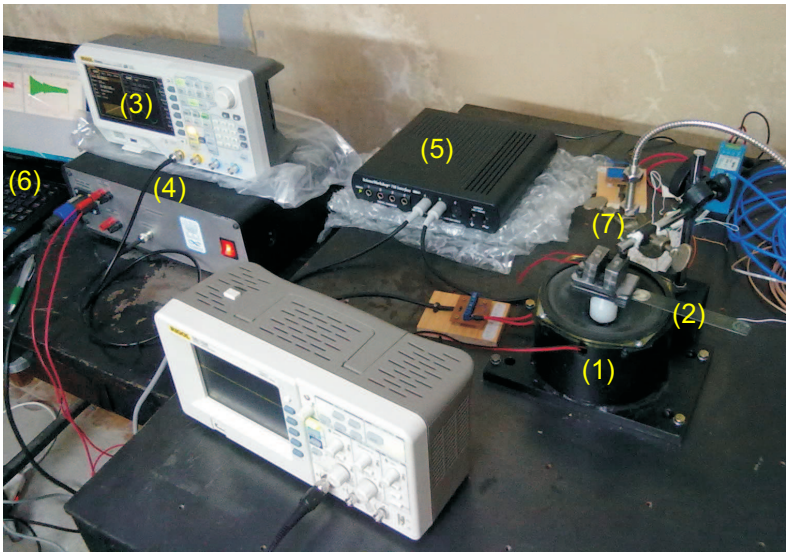

Figure 2: Experimental setup for the proposed system.

response function FRF (in units of $g = 9.81m/s^2$). The results are presented for different values of the resistive load to emulate different load conditions. The effective load resistance is the equivalent resistance of the resistive load used and $R = 984\text{k}\Omega$, which is the input resistance of the data acquisition system which is seen in parallel with the resistive load. This implies $R_e = 1/(1/R + 1/R_{ad})$ are presented in Table 2.

The voltage and power FRFs for the first mode are presented in Figs. (3) and (4) . The damping coefficient of the first mode was set to $\xi_1 = 0.02$ to fit the voltage generation for the large resistive load. The damping for the second mode is given by the relation: $\xi_2 = \xi_1\omega_1/\omega_2$

Figure (3) presents voltage generation in the nearness of the first mode of the system, for the whole set of considered resistances. It can be observed a perfect agreement between the theoretical (numerical) and experimental results. The maximum value of V/g is $\sim 4.8\text{V/g}$ and is for the maximum load resistance. The minimum, instead, is approximately of 0.08V/g and is for the lowest resistance ($9.85\text{k}\Omega$) which is the case of maximum current consumption.

The electrical power generated can be observed in Fig. (4). There, the different curves show the electrical power for the considered resistances. The maximum generated power is for resistance $R = 986\text{k}\Omega$ and it is 0.025mW. For a better presentation of the results, we only show here the numerical curves only. However, we have also a very good agreement for the other cases.

Table 2: Effective load resistance which is the parallel between the used (measured) resistance and $R = 986k\Omega$ (input resistance of the data acquisition system).

R (measured)	R_e(effective)
-	986 kΩ $(986 \times 10^3\Omega)$
331 kΩ	247.8 kΩ
98.6 kΩ	89.6 kΩ
32.8 kΩ	31.7 kΩ
9.95 kΩ	9.85 kΩ

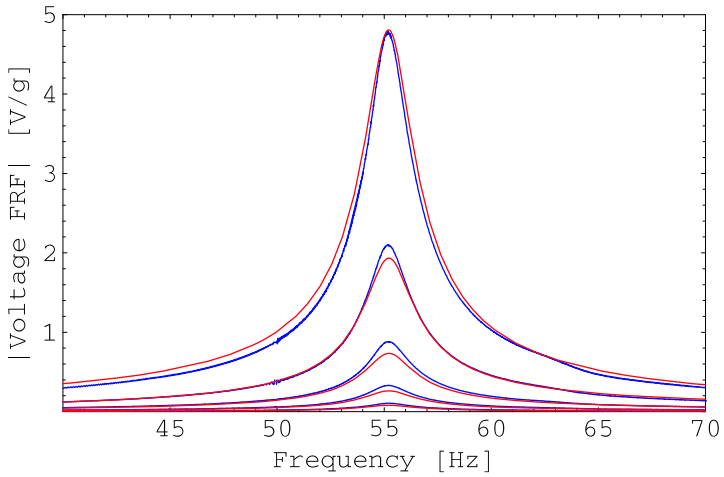

Figure 3: FRFs for frequencies near the first mode of the piezoelectric beam for a given set of resistors. Blue lines experimental, red lines theoretical.

Figures (5) and (6) show the results for the generated voltage and power for frequencies near the second mode of the system. Surprisingly, we can see in this case that the generated voltage (see Fig. 5) is greater than the case for the first mode. The maximum voltage is about $\sim 6.1V/g$, almost 30 % above the voltage for the first mode. The minimum voltage, instead, is $0.52V/g$ which is more than six times the voltage generated for the first mode. Regarding the generated power, from Fig. (6) it is possible to observe a maximum generated power of $0.15\mathrm{mW}$ for a resistance of $R = 98.6\mathrm{k}\Omega$. Note that this value is different from the value obtained in the case of the first mode.

An interesting question that immediately arises is why there exist differences in the generated voltage between the first and second mode that obviously affects the generated power. The answer can be appreciated in Table (3). From expression (1) is possible to see that the generated voltage is directly proportional to the electromechanical coupling θ and Γ which is proportional to the mode integral. Since Γ is equal for both modes, the difference in the generated voltage is caused by the electromechanical coupling θ. The electromechanical coupling depends on the attachment place of the piezoelectric disc and on the first derivative of the analyzed mode evaluated at the span of the piezoelectric disc (see Eq. 18 in (14)). If one wants to generate a large voltage it is necessary to find the way to maximize $e_{zx} = d_{31}c_{11}^E$ (where d_{31} is the piezoelectric constant and c_{11}^E is the Young modulus of the piezoelectric element) or $\phi_j'(L_1)$ which is the first derivative of the corresponding mode at the span of the piezoelectric disc.

From Table (3) it is possible to see that θ for the second mode is more than eight times larger compared with the first mode. Therefore, since e_{zx} depends on the physical constants of the

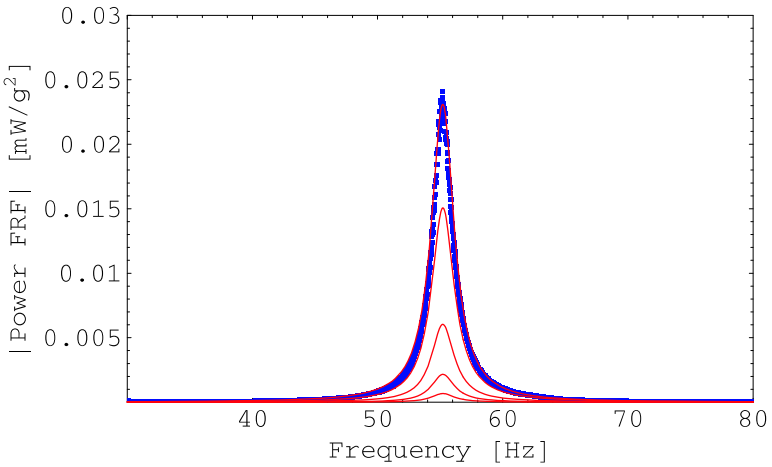

Figure 4: Generated electrical power for frequencies near the first mode of the piezolectric beam of Fig. 3. Blue lines experimental, red lines theoretical.

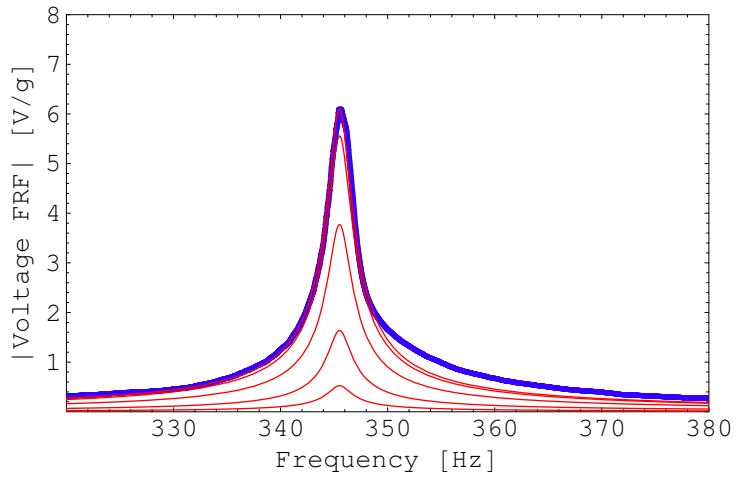

Figure 5: FRFs for frequencies near the second mode of the piezoelectric beam for a given set of resistors.

piezoelectric disc, the difference in the generated voltage comes from differences in $\phi_j'(L_1)$ for both modes.

Another interesting question has to be with optimum load resistance, i.e. the resistance that maximizes power. It has been previously mentioned in this work that this load resistance varies depending on the mode. From the expression of voltage and power P, ($P = V^2/R$) it is possible to mathematically obtain the value of R that maximizes power. It is straightforward to show that this optimum load is:

$$R = \frac{\omega_j^4 + (4\xi_j^2 - 2)\omega_j^2\Omega^2 + \Omega^4}{\sqrt{\Omega^2(\theta_j^4 + 2C\theta_j^2(\omega_j^2 - \Omega^2)) + C^2(\omega_j^4 + (4\xi_j^2 - 2)\xi_j^2\Omega^2 + \Omega^4)}} \tag{3}$$

In the case of the values of table 3, this expression reduces to:

$$R = \frac{1}{C\Omega} \tag{4}$$

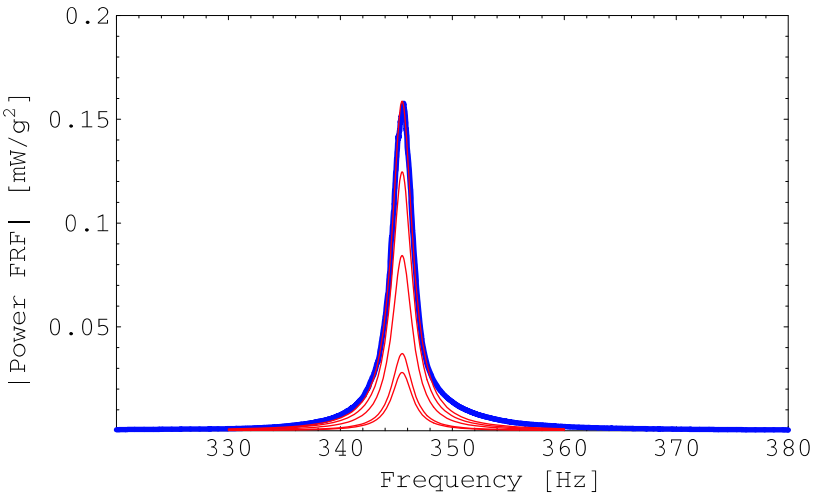

Figure 6: Generated electrical power for frequencies near the second mode of the piezoelectric beam of Fig. 7.

Table 3: Physical parameters of the prototype device consisting in a steel beam and a piezoelectric disc used for the experiments

mode	ξ_j	ω_j	θ_j	Γ_j	V/g(max)	V/g(min)	Power [mW]
1	0.02	346.96	0.000129	0.09	4.8	0.08	0.023
2	0.0032	2170.9	0.000804	0.094	6.1	0.52	0.16

Therefore, the optimum load resistance R diminishes as one considers higher modes of vibration (higher excitation frequencies) as $1/\Omega$. In Figures (7a) and (b) it is possible to observe the calculated optimum load resistance for both modes using the exact (Eq. 3) and the (Eq. 4) approximated formula. The coincide between both expressions is evident. Additionally, it can be seen that $R = 7.205 \times 10^5$ for the first mode and $R = 1.1515 \times 10^5$ for the second mode. Obviously these values do not coincide with those obtained in the experiments since the they were made for a finite set of resistances.

4 CONCLUSIONS

In this work we made a series of dynamic experiments of a new type of lead free piezoelectric material. From these experiments we conclude the following items.

- This new type of material, originally made for other purposes, can be used for energy harvesting when attached to a vibrating element such as a beam or another flexible structure.
- The agreement between numerical and experimental results show that the employed analytical model is appropriate to describe the electromechanical system.
- Regarding the generation of voltage, the values obtained in the experiments was acceptable. Compared with other commercial piezoelectric materials such as PZT, the generation was lower. However, there exists several parameters of this new material that can be optimized to obtain a larger voltage. For example, this may be achieved by optimizing the physical dimensions of the piezoelectric disc.

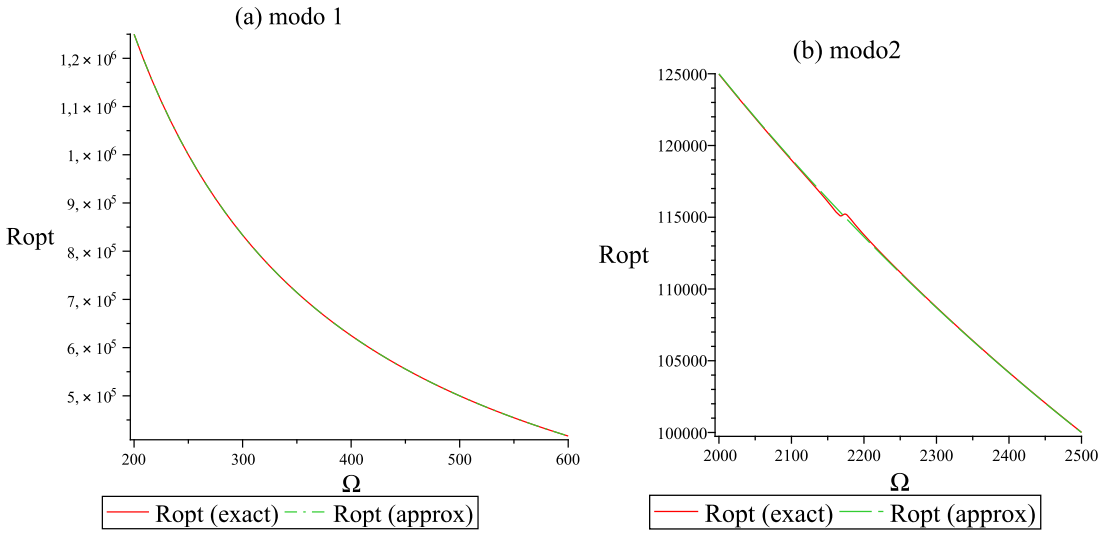

Figure 7: Optimum load resistance R for (a) frequencies near the first mode of the system and (b) frequencies near the second mode of the system.

- In the particular case of the considered system and ceramic characteristics such as density and composition of the main phase, the maximum power generation is for the second mode with a ten times larger power compared to the first mode. The reason of this behavior is due to the electromechanical coupling which depends on the attachment position of the piezoelectric disc over the beam.

ACKNOWLEDGEMENTS

M. Febbo acknowledges CONICET and Secretaría de Ciencia y Tecnología UNS. S. P. Machado acknowledges CONICET and Secretaría de Ciencia y Tecnología UTN FRBB.

REFERENCES

[1] Y. C. Shu and I. C. Lien, 2006, Efficiency of energy conversion for a piezoelectric power harvesting system, J. Micromech. Microeng. 16, 2429:2438.

[2] S. R. Anton, and Sodano H. A., 2007, A review of power harvesting using piezoelectric materials (2003-2006), Smart Mater. Struct. 16:R1-R21.

[3] Sodano H A, Inman D J and Park G, 2004, A review of power harvesting from vibration using piezoelectric materials, Shock Vib. Dig. 36, 197:205.

[4] Y.B. Jeon, R. Sood, J. H. Jeong and S. G. and Kim, 2005, MEMS power generator with transverse mode thin film PZT, Sensors Actuators A 122, 16:22.

[5] G. Poulin G, E. Sarraute and F. Costa, 2004, Generation of electric energy for portable devices: comparative study of an electromagnetic and a piezoelectric system, Sensors Actuators A 116, 461:71.

[6] S. Roundy, P. K. Wright and J. Rabaey, 2003, A study of low level vibrations as a power source for wireless sensor nodes, Comput. Commun. 26, 1131:1144.

[7] X. Pang, J. Qiu, K. Zhu, J. Luo, 2011, Study on the sintering mechanism of KNN-based lead-free piezoelectric ceramics, J. Mater. Sci. 46, 2345:2349.

[8] A. Thongtha, T. Bongkarn, 2011, Optimum Sintering Temperature for Fabrication of $0.8Bi_{0.5}Na_{0.5}TiO_{3-0.2}Bi_{0.5}K_{0.5}TiO_3$ Lead-Free Ceramics by Combustion Technique Eng.

Mater. 474, 1754:1759.

[9] H. Wang, R. Zuo, Y. Liu, J. Fu, 2010, Densification behavior, microstructure, and electrical properties of sol gel derived niobium-doped $(\mathrm{Bi}_{0.5}\mathrm{Na}_{0.5})0.94\mathrm{Ba}_{0.06}\mathrm{TiO}_3$ ceramics, J. Mater. Sci. 45, 3677:3682.

[10] L. Ramajo, R. Parra, M.A. Ramírez, M.S. Castro, 2011, Electrical and Microstructural Properties of CaTiO_3-doped $\mathrm{K1/2Na1/2NbO}_3$-Lead Free Ceramics, Bull. Mater. Sci. 34, 1213:1217.

[11] H. Birol, D. Damjanovic, N. Setter, 2006, Preparation and characterization of $(\mathrm{K}_{0.5}\mathrm{Na}_{0.5})Nb\mathrm{O}_3$ ceramics, J. Eur. Ceram. Soc. 26, 861Ű866.

[12] Y. Saito, H. Takao, T. Tani, T. Nonoyama, K. Takatori, T. Homma, T. Nagaya, M. Nakamura, 2004, Lead-free piezoceramics, Nature 432, 84:87.

[13] F. Rubio-Marcos, J.J. Romero, M.S. Martín-Gonzalez, J.F. Fernández, 2010, Effect of stoichiometry and milling processes in the synthesis and the piezoelectric properties of modified KNN nanoparticles by solid state reaction, J. Eur. Ceram. Soc. 30, 2763:2771.

[14] S. P. Machado, M. Febbo, S. Bellizzi, Piezoelectric energy harvesting from superior modes, ENIEF 2014, in press.

[15] A. Erturk, and D. J. Inman, 2009, An experimentally validated bimorph cantilever model for piezoelectric energy harvesting from base excitations, Smart Mater. Struct. 18, 025009.